9328 *Biochemistry* **2010,** *49,* 9328–9338
DOI: 10.1021/bi100841u

BIOCHEMISTRY
including biophysical chemistry & molecular biology
Article

Acid-Induced Aggregation of Human Monoclonal IgG1 and IgG2: Molecular Mechanism and the Effect of Solution Composition

Sanjay B. Hari,[‡,§] Hollis Lau,[‡] Vladimir I. Razinkov,[‡] Shuang Chen,[‡,∥] and Ramil F. Latypov*[,‡]

[‡]*Process and Product Development, Amgen Inc., Seattle, Washington 98119, United States,* [§]*Department of Chemistry, University of Washington, Seattle, Washington 98195, United States, and* [∥]*School of Chemical Engineering, Purdue University, West Lafayette, Indiana 47907, United States*

Received May 25, 2010; Revised Manuscript Received September 3, 2010

ABSTRACT: The prevention of aggregation in therapeutic antibodies is of great importance to the biopharmaceutical industry. In our investigation, acid-induced aggregation of monoclonal IgG1 and IgG2 antibodies was studied at pH 3.5 as a function of salt concentration and buffer type. The extent of aggregation was estimated using a native cation-exchange chromatography (CEX) method based on the loss of soluble monomer. This approach allowed quantitative analysis of antibody aggregation kinetics for individual and mixed protein solutions. Information regarding the aggregation mechanism was gained by assessing stabilities of intact antibodies relative to their Fc and Fab fragments. The role of protein thermodynamic stability in aggregation was deduced from differential scanning calorimetry (DSC). The rate of aggregation under conditions mimicking the viral inactivation step during monoclonal antibody (mAb) processing was found to be strongly dependent on the antibody subclass (IgG1 vs IgG2). At 25 °C, IgG1s were resistant to low pH aggregation, but IgG2s aggregated readily in the presence of salt. The observed distinction between IgG1 and IgG2 aggregation resulted from differential stability of the corresponding C_H2 domains. This was further confirmed by experimenting with an IgG1 molecule containing an aglycosylated C_H2 domain. Interestingly, comparative analysis of two buffer systems (based on acetic acid vs citric acid) revealed differences in mAb aggregation under identical pH conditions. Evidence is provided for the importance of the total acid concentration for antibody aggregation at low pH. The effects of C_H2 instability and solution composition on aggregation are significant and deserve careful consideration during the development of mAb- or Fc-based therapeutics.

Understanding and preventing protein aggregation are of great importance to the biopharmaceutical industry. Aggregation of therapeutic antibodies that occurs during development may lead to unacceptable levels of particulate matter, loss of biological activity, and even adverse reactions *in vivo* (*1*−*6*). Protein therapeutics may be subjected to a large variety of stress conditions upon purification, formulation, storage, and delivery. One of the stress factors most typically experienced by monoclonal antibodies (mAbs)[1] is the low pH treatment used to elute bound proteins from affinity resins and during the viral inactivation step (*7*). mAbs with high affinity and specificity are now widely used in human therapy, and more new constructs are being developed. Therefore, a basic understanding of acid-induced aggregation is critical for the reduction or elimination of mAb aggregation issues during the manufacture of biotherapeutics. However, providing a molecular level description of mAb aggregation is analytically challenging and time-consuming because of the large size of antibodies (∼150 kDa). Therapeutic IgG1 and IgG2 mAbs are multidomain and multichain glycosylated proteins exhibiting significant heterogeneity in structure and stability (*8*−*11*). Since the Fc and Fab regions of mAbs bear different stability and surface properties, they may not contribute equally toward aggregation induced by low pH. Clarifying the role of these regions in antibody aggregation is important for engineering mAb-based therapeutics with improved stability.

Although the effect of acidic conditions on antibody structure, stability, and folding has been thoroughly investigated (*7*, *12*−*16*), there is little information regarding the aggregation of different subclasses of mAbs (IgG1, IgG2, etc.). It is interesting to note that some studies reveal significant antibody aggregation at low pH (*14*), whereas others fail to observe any measurable aggregation under fairly similar conditions (*7*). The specific role of the Fc and Fab regions in the low pH aggregation process also has not been fully addressed. Furthermore, protein aggregation studies may be confounded by the fact that the observed differences may result from variations in the experimental conditions rather than the intrinsic properties of antibodies. Specifically, the effects of solvent composition (buffer type, ionic strength, etc.) on the rate and extent of antibody aggregation can be significant (*17*).

The role of an IgG subclass in heat-induced aggregation and degradation of mAbs has been recently evaluated by Ishikawa et al. (*18*). The authors compared stability of IgG1, IgG2, and IgG4 subclasses as a function of pH (4.0−7.0) and 40 °C storage. The study revealed clear differences in the physical and chemical degradation of the various IgGs under low-salt conditions. Specifically, IgG1s were found to be more susceptible to fragmentation,

*To whom correspondence should be addressed. E-mail: rlatypov@amgen.com. rlatypov@live.com. Phone: (206) 265-8851. Fax: (206) 217-0346.

[1]Abbreviations: aglyco-IgG1, aglycosylated IgG1; CEX, cation-exchange chromatography; CEX52, cation-exchange chromatography at pH 5.2; C_H2 or C_H3 domains, constant domains comprising the Fc portion of IgG; DFP, diisopropyl fluorophosphate; DSC, differential scanning calorimetry; Fab, fragment antigen binding; Fc, fragment crystallizable; IgG, immunoglobulin G; mAb, monoclonal antibody; p*I*, isoelectric point; UV Abs, absorbance in the UV region.

 Published on Web 09/15/2010

whereas IgG4s were more susceptible to aggregation. In a related study, Franey et al. probed the importance of the antibody subclass (IgG1 vs IgG2) in mAb aggregation under neutral pH and mildly elevated temperature (*19*). They found that IgG2s aggregated slightly faster than IgG1s in correlation with the increased amounts of free cysteines in these molecules. However, it remained unclear as to what regions (or domains) were responsible for aggregation and how they would respond to solution acidification. In another new study, Sahin et al. have evaluated stability and aggregation of IgG1s at pH values ranging from 3.5 to 6.5 (*20*). In contrast to the two publications referenced above, these experiments employed denaturing temperatures resulting in a rapid aggregation process influenced by protein thermal unfolding.

In this work, we sought to measure aggregation kinetics for the two most common IgG subclasses used in biotechnology: IgG1 and IgG2. The experiments were optimized to produce 25 °C aggregation data within a short period of time with minimal contributions from chemical degradation processes. To differentiate less stable mAbs from their more stable counterparts, preference was given to analyzing mAb mixtures over individual protein samples. This was made possible by applying our recently developed CEX-based methodology for studying mAb aggregation behavior (*21*, *22*). The role of protein thermodynamic stability in aggregation was investigated by employing DSC. All experiments were performed in two different buffer systems commonly used in mAb processing: acetate and citrate. Results of the present work provide compelling evidence for the importance of antibody subclass, ionic strength, and total acid concentration. The contribution of various IgG domains to low pH aggregation was clarified, allowing more detailed insight into this degradation process.

MATERIALS AND METHODS

High-purity recombinant human monoclonal IgG1 and IgG2 antibodies were produced at Amgen Inc. Fc and Fab fragments of IgG2-A were purified as previously described (*22*). Endoproteinase Lys-C was purchased from Roche (Basel, Switzerland). Diisopropyl fluorophosphate (DFP) was purchased from Calbiochem (La Jolla, CA). All other reagents and chemicals were of analytical grade or better. All solutions were 0.22 μm filtered prior to use.

Cation-Exchange Chromatography at pH 5.2 (*CEX52*). The CEX52 method (*21*) was run on an UltiMate 3000 Series (Dionex, Sunnyvale, CA) HPLC system. Chromatography was performed on a ProPac WCX-10 analytical column (weak cation exchange, 4 × 250 mm; Dionex) preceded by a ProPac WCX-10G guard column (weak cation exchange, 4 × 50 mm; Dionex) at 25 °C. Protein samples were loaded onto the column and analyzed at a flow rate of 0.7 mL/min. The column was equilibrated with buffer A (20 mM sodium acetate−NaOH, pH 5.2), and protein was eluted with a linear gradient of buffer B (20 mM sodium acetate−NaOH, 300 mM NaCl, pH 5.2) from 0% to 100% over 35 min. Following elution, the column was washed with buffer C (20 mM sodium acetate−NaOH, 1 M NaCl, pH 5.2) for 5 min and reequilibrated with buffer A for 16 min. Absorbance was measured at 215 and 280 nm. Integration percentages were calculated relative to $t = 0$ or controls incubated at pH 5.0, as appropriate.

Differential Scanning Calorimetry (*DSC*). Protein solutions used for DSC had the same solution composition as the "high-salt" samples described below. DSC measurements were taken using a VP-Capillary DSC system (MicroCal Inc., Northampton, MA) equipped with tantalum 61 cells, each with an active volume of 125 μL. The pH of protein samples was adjusted to 3.5 immediately prior to DSC measurements to minimize protein aggregation. The mAbs were tested individually at a protein concentration of 0.5 mg/mL, and a buffer control without protein was used as a reference. The samples were scanned from 20 to 90 °C at a rate of 20 °C/h following an initial 15 min equilibration at 20 °C. A filtering period of 16 s was used, and the data were analyzed using Origin 7.0 software (OriginLab Corp., Northampton, MA). Resulting thermograms were corrected by subtraction of buffer control scans. The corrected thermograms were normalized for protein concentration.

Aggregation Experiments. For protein mixtures, antibodies were initially dialyzed against 10 mM sodium acetate−NaOH, pH 5.0, and the resulting solutions were used in subsequent sample preparations. Due to low sample quantity, the aglycosylated IgG1 (aglyco-IgG1) and its glycosylated variant were not dialyzed but added directly from a stock solution composed of 10 mM sodium acetate−NaOH, pH 5.2, and 9% (w/v) sucrose into a final pH 3.5 mixture. The same procedure was applied in the case of the Fc and Fab fragments of IgG2-A.

Three sample types were made for each protein mixture based on final pH and NaCl concentration: controls (in 10 mM sodium acetate−NaOH, pH 5.0), "low-salt" samples (in 0 M NaCl, pH 3.5), and "high-salt" samples (in 0.5 M NaCl, pH 3.5). The final concentration of each protein was 1 mg/mL. Low pH samples were adjusted to pH 3.5 using either acetic (10% (v/v), 1.75 M) or citric (10% (w/v), 520 mM) acid. The amount of acid required to achieve the desired pH was determined in separate experiments. The acid was quickly mixed to minimize protein exposure to local regions of extreme acidity. In order to adjust the ionic strength and maintain a pH of 3.5 for samples using citric acid, sodium hydroxide (10 N) was added to the acid, and the resulting solution was added to the protein mixture. Samples were protected from light and incubated for up to 2 days at 25 °C without agitation. Sample aliquots were taken at predetermined intervals, usually after 0, 2, 4, 24, and 48 h of incubation. The aliquots were immediately analyzed by CEX52 or stored on ice prior to analysis, i.e., under conditions minimizing further aggregation.

Protein concentration dependence of low pH mAb aggregation was measured at 25 °C in a citrate−NaOH buffered solution at pH 3.7. Concentrated IgG2-B (71.2 mg/mL) was diluted down to 0.5, 1.0, 3.0, and 5.0 mg/mL in a solution with the following final composition: 80 mM citrate−NaOH, 0.5 M NaCl. The samples were protected from light and incubated for up to 12 h without agitation. Sample aliquots were taken at predetermined intervals and analyzed by CEX52 as described above.

Limited Proteolysis of Aglyco-IgG1 and Its Glycosylated Variant Using Endoproteinase Lys-C. Fc and Fab fragments from aglyco-IgG1 and its glycosylated variant were obtained by limited proteolysis using endoproteinase Lys-C (*21*−*23*). The antibody samples were diluted to a concentration of 1.2 mg/mL in 100 mM Tris-HCl, pH 7.5, and incubated with Lys-C at an enzyme-to-substrate ratio of 1:200 (w/w) at 37 °C for 10 min. The protease inhibitor, diisopropyl fluorophosphate (DFP, 1 mM), was added to the digested samples, followed by the addition of NaCl to a concentration of 0.5 M. Then, acetic acid was added to a final concentration of 160 mM to achieve pH 3.5 and to yield a protein concentration of 1 mg/mL. The samples were incubated at 25 °C as described above.

Kinetic Modeling. An extended Lumry−Eyring model has been previously proposed to study the kinetics of irreversible

protein aggregation (*5*, *24*−*26*). The model includes both folding−unfolding transitions and association and assembly processes. The aggregation kinetics can exhibit apparent first- or second-order features depending on the detailed aggregation mechanism and the rate controlling step(s) in the aggregation process (*25*, *26*). The model used in this study was cast in terms of the rate of loss of total (soluble) monomer, *N*, which can be measured experimentally using CEX52. For comparison purposes, [N] was normalized and expressed as dimensionless concentration (%).

When the characteristic time scale of unfolding (denaturation) is significantly longer than that of association and aggregation, nonnative monomers are consumed immediately upon formation. Unfolding becomes the rate-determining step, resulting in apparent first-order kinetics with the following rate expression for [N]:

$$\frac{d[N]}{dt} \approx -k_u[N] = -k_{obs}[N]$$

where k_u is the unfolding rate constant and k_{obs} is the observed (apparent) rate constant.

The normalized concentration of *N* (%) in this case exhibits exponential decrease as a function of time and can be described as

$$[N] = 100e^{-k_{obs}t}$$

The aggregation process exhibits pseudo-second-order behavior if the rate-determining step is protein−protein association, in which case the rate expression is

$$\frac{d[N]}{dt} = -k'_{obs}[N]^2$$

For second-order kinetics, the normalized concentration of *N* (%) is described by the expression:

$$[N] = \frac{1}{k'_{obs}t + \frac{1}{100}}$$

The rate constant k'_{obs} is obtained from the slope of 1/[N] − 1/100 as a function of time, *t*, since

$$k'_{obs}t = \frac{1}{[N]} - \frac{1}{100}$$

Both first- and second-order kinetic models were evaluated for fitting the aggregation data, and the results are presented in the Results and Discussion section.

RESULTS AND DISCUSSION

Description of the Experimental Design and Sample Composition. The main goal of our investigation was to generate aggregation data over a short period of time while minimizing chemical protein degradation. Our previous low pH studies indicated an acceleration of mAb aggregation at 25 °C compared to 4 °C (*22*), and higher temperatures were expected to accelerate it further. However, there is a known risk of increased protein hydrolysis at low pH and elevated temperature (*27*). Therefore, 25 °C was considered the optimal temperature for the purpose of this study. Ionic strength was also recognized as an important factor because of increased charge−charge repulsion between proteins under acidic conditions. We performed screening experiments in the presence of 0−1 M NaCl (results not shown) and found that 0.5 M salt was adequate for achieving substantial aggregation within only 1−2 days at pH 3.5 (see below). Buffer composition (acetate vs citrate) was used as another variable for assessing buffer-specific modulation of mAb aggregation. In both cases, the final pH was brought to the same value of 3.5. However, due to the difference in pK_a between acetic and citric acid, the samples were prepared with different final acid concentrations: they required 50 mM acetic acid to achieve pH 3.5 and only 5 mM citric acid to reach the same point. Correspondingly, protein aggregation data were generated using either 50 mM acetic acid or 5 mM citric acid. These samples were further differentiated by the presence or absence of 0.5 M NaCl and were denoted as the "high-salt" and "low-salt" samples, respectively (see Materials and Methods for more details).

Table 1: Antibody Samples Used in Real-Time Aggregation Experiments at pH 3.5

mixture	antibody	IgG subclass	p*I*
1	IgG1-A	IgG1	8.9
	IgG2-A	IgG2	8.8
	IgG2-B	IgG2	6.8
2	IgG1-B	IgG1	9.0
	IgG2-D	IgG2	8.7
	IgG2-E	IgG2	7.0
3	IgG1-C	IgG1	8.7
	aglyco-IgG1	IgG1	7.6
	IgG2-C	IgG2	7.8
4	IgG1-D	IgG1	8.8
	IgG2-F	IgG2	8.1
	IgG2-G	IgG2	8.0
	IgG2-H	IgG2	7.2
5[a]	IgG1-A	IgG1	8.9
	IgG1-B	IgG1	9.0
	IgG2-B	IgG2	6.8
	IgG2-C	IgG2	7.8
6	IgG2-I	IgG2	8.3
	IgG2-J	IgG2	8.0
7[b]	IgG1-E	IgG1	9.1

[a]This mixture includes mAbs that are also present in mixtures 1, 2, and 3. [b]This is the only sample which contained a single mAb.

Aggregation Kinetics of IgG1 and IgG2 mAbs at pH 3.5. Working with protein mixtures ensures that each protein experiences identical conditions, which allows investigation of intrinsic differences in the IgG1 and IgG2 aggregation (*22*). Among the 16 antibodies tested, 6 molecules were of the IgG1 and 10 molecules of the IgG2 subclass (see Table 1). Besides the expected difference in the hinge region sequence, all IgG1s and IgG2s were similar in size and structure but varied greatly in overall p*I* (6.8−9.1). With the exception of aglyco-IgG1, all mAbs were fully glycosylated at Asn297, which is the conserved glycosylation site in the C_H2 domains of both IgG1s and IgG2s. Inclusion of aglycosylated IgG1 in this study provided a direct assessment of the role of C_H2 glycosylation in antibody stability and aggregation (*28*).

Because of our desire to compare IgG1s and IgG2s under identical conditions, most of the mixtures included both IgG subclasses (Table 1). However, this was not always possible since we could only mix proteins with nonoverlapping CEX52 profiles. For example, IgG1-E was tested individually, and one of the mixtures contained only two IgG2s (IgG2-I and IgG2-J) and no IgG1s. Due to the large number of different mAbs, a complete combinatorial analysis was impractical, and a comparison of individual against mixed IgGs was not performed. This experimental strategy was justified since it has been previously demonstrated that little to no interference occurs between different IgGs (*22*). To further test the validity of this assumption, one of

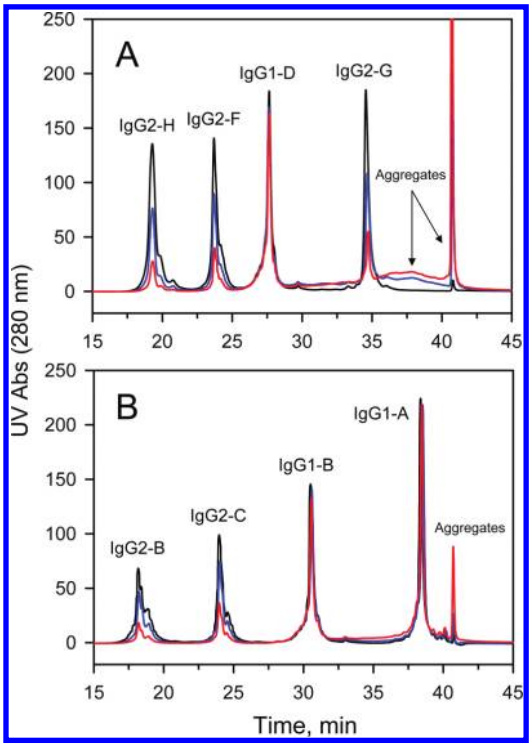

FIGURE 1: CEX52 results for mAb mixtures 4 (A) and 5 (B) (see also Table 1) incubated at pH 3.5 in the presence of 50 mM acetic acid and 0.5 M NaCl. The protein solutions were protected from light and incubated at 25 °C for up to 48 h without agitation. The black, blue, and red traces correspond to 0, 4, and 24 h time points, respectively. In (A), soluble aggregates accumulated in significant amounts, but they were readily identified and manually excluded from peak analysis. The results show that IgG1s are more resistant to aggregation than IgG2s under identical conditions.

the mixtures was composed of 4 mAbs that were randomly distributed between 3 other mixtures (see mixture 5 in Table 1). Results for these molecules varied insignificantly (see below), providing additional support for our experimental design.

The CEX52 overlays shown in Figure 1 illustrate mixtures 4 and 5, the only two 4-mAb mixtures tested in this study. In both cases, there was sufficient separation between different IgGs, facilitating peak identification and integration. There was a dramatic change in the peak area for some of the mAbs after 4 and 24 h of incubation, which reflected the loss of native monomer due to aggregation. Also, Figure 1 provides evidence for the formation of protein aggregates eluting at higher salt concentrations (see Chen et al. (*22*) for more information). Generally, the aggregates eluted at ~41 min, corresponding to the beginning of the column washing step with 1 M salt (see Materials and Methods). In several cases though, the aggregates eluted earlier (between 30 and 40 min) and overlapped with some late eluting mAbs (Figure 1A). However, they were easily identified by the characteristically broad peak shape and excluded from peak analysis.

It has been demonstrated that the loss of native monomer as measured by CEX52 represents an indirect measure of protein aggregation (*22*). Following incubation at pH 3.5, we collected 0−48 h snapshots for all 16 mAbs as a function of solution composition. Figure 2 compares aggregation kinetics for a representative set of proteins incubated in the acetate and citrate solutions with and without 0.5 M NaCl. It is evident that no significant antibody aggregation occurred in the absence of salt within 2 days of incubation. However, the addition of NaCl greatly accelerated aggregation of IgG2s and aglycosylated IgG1. The latter exhibited some aggregation during sample preparation even under low-salt conditions but aggregated almost instantaneously and completely when salt was present. Further details of aglyco-IgG1 aggregation are discussed in a subsequent section. In general, IgG1s showed little to no aggregation even in the presence of salt as illustrated by the IgG1-A data in Figure 2, whereas the dependency of IgG2-F aggregation on solution composition was a characteristic of all IgG2s.

The consistency and reproducibility of the aggregation data generated by CEX52 are illustrated in Figure 3. It is striking to see how similar the results are in the case of the different mAb mixtures. This feature indicates little interference between proteins even under such destabilizing conditions as pH 3.5, in agreement with our previous results (*22*).

Mixing IgG1s and IgG2s together provided unequivocal evidence for the importance of the antibody subclass in aggregation: the finding that IgG2s aggregated more readily under low pH conditions held true for all tested mAbs. Subsequently, DSC measurements were performed under similar high-salt conditions to assess the role of protein conformational stability in aggregation (see Figure 4 and Table 2). Figure 4A compares DSC profiles of IgG1-A, IgG2-A, and IgG2-B, the same mAbs that were previously tested at pH 6.8 (see Figure 3A in Chen et al. (*22*)). There is a dramatic change in the relative stability of the various IgG domains when the pH is lowered from 6.8 to 3.5. The largest destabilization is exhibited by the C_H2 domains as they begin to melt at as low as ~30−40 °C. This is in agreement with the fact that C_H2 domains are only marginally stable under acidic conditions (*29*, *30*). At pH 3.5, their DSC transitions are fully separated from other peaks greatly facilitating analysis. In contrast, the Fab and C_H3 domains melt at higher temperatures (~50−80 °C), giving rise to complex profiles ranging from a single major transition to multiple overlapping transitions (see Figure 4B−D). We chose not to focus on these domains and proceeded with the more straightforward analysis of C_H2 denaturation.

As seen from Table 2, there is a clear difference in thermal stability between the IgG1 and IgG2 C_H2 domains. The average apparent IgG1 melting temperature (T_m), as measured in the acetate buffer, is 42.6 ± 2.1 °C. The corresponding value for IgG2s is only 35.0 ± 2.3 °C, which is 7.6 °C lower. A similar observation is made in the case of the citrate samples, which show an average T_m difference of 7.3 °C. Therefore, the disparity between IgG1 and IgG2 aggregation is consistent with the fact that IgG2 C_H2 domains are less stable than their IgG1 counterparts.

Aggregation Kinetics of the Fc and Fab Fragments of IgG2-A at pH 3.5. Previously, we identified some problems in correlating DSC results with CEX aggregation data (*22*). One issue stems from the fact that IgG1s and IgG2s are composed of one Fc region and twice as many Fabs. Despite the fact that C_H2 is the least stable domain at pH 3.5 (Figure 4), it is possible that moderate instability in the Fabs could have an impact on aggregation because of their higher effective concentration. In other words, the presence of a less stable C_H2 may not necessarily mean that changes in this region determine the rate of aggregation. Another issue is that simply knowing the order of melting transitions is not sufficient for predicting antibody aggregation. For example, we observed that in some cases Fab fragments may have a greater aggregation propensity despite being more thermodynamically stable (*22*). Similarly, Kameoka et al. (*17*) previously concluded that differences in the aggregation propensity of IgG in various buffers could not be fully explained by the DSC results.

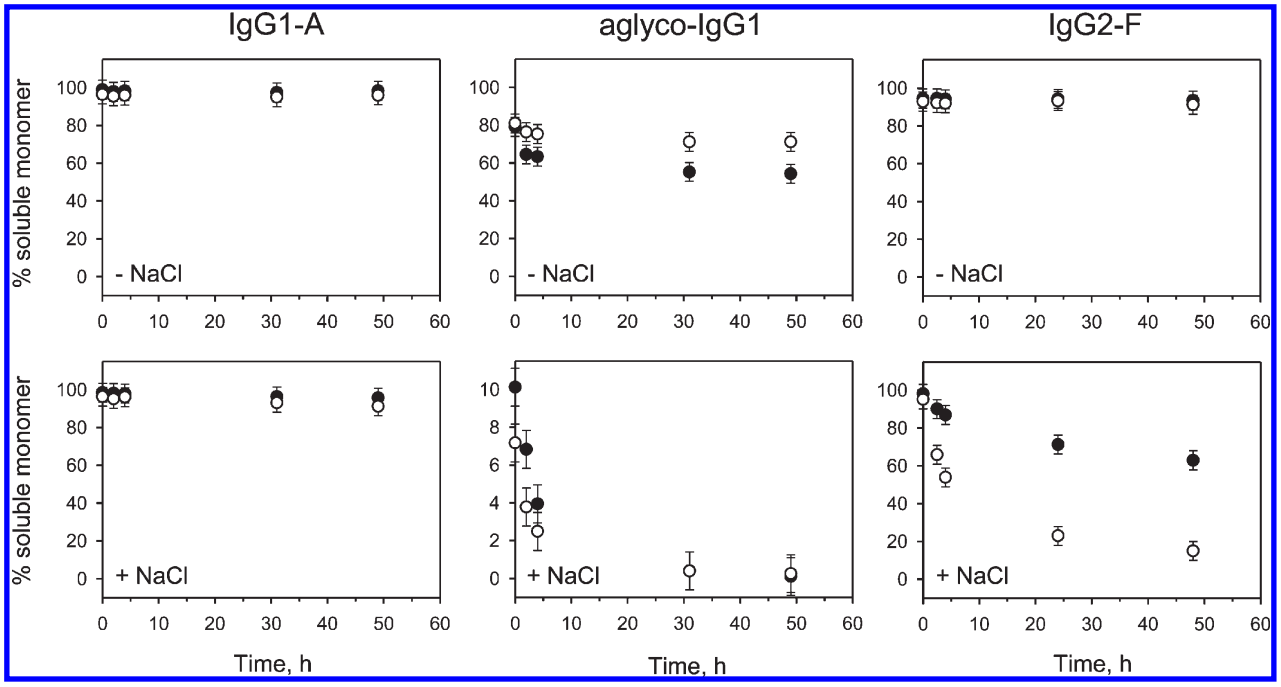

FIGURE 2: Aggregation kinetics for a representative set of proteins incubated at pH 3.5 in acetic acid (50 mM) or citric acid (5 mM) solutions with and without 0.5 M NaCl. Open and closed symbols correspond to acetic acid and citric acid samples, respectively. Samples with 0 (−) and 0.5 M (+) NaCl are shown in the upper and lower sets of panels, respectively. All IgG1 results generated in this work are comparable to the IgG1-A data on the left. The aglyco-IgG1 (middle panels) lacks C_H2 glycosylation and represents the most unstable molecule in this study. Note that an expanded scale is used to illustrate its aggregation in the presence of 0.5 M NaCl. The IgG2-F data on the right are shown to illustrate the behavior of the ten IgG2s tested. The error bars were calculated from the standard deviation of replicate injections over several runs.

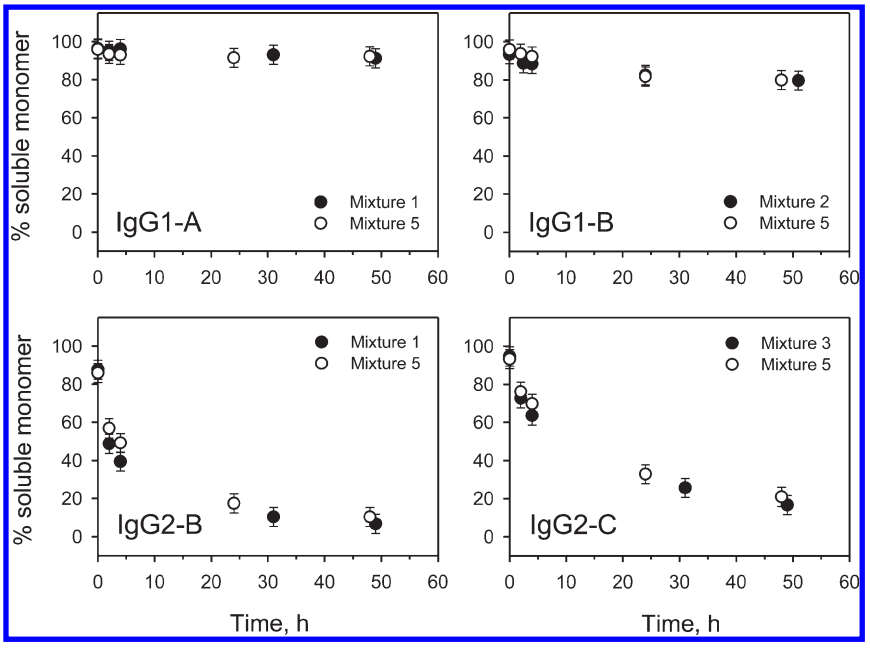

FIGURE 3: Aggregation kinetics of IgG1-A, IgG1-B, IgG2-B, and IgG2-C measured in the case of different mAb mixtures. In all cases, the proteins were incubated at pH 3.5 in 50 mM acetic acid with 0.5 M NaCl. Open and closed symbols correspond to protein aggregation results for the different mixtures as indicated (see Table 1 for details). The error bars were calculated from the standard deviation of replicate injections over several runs.

We have already provided justification for the use of Fc and Fab fragments in the identification of aggregation-prone regions in mAbs (*22*). The same strategy was employed here to gather evidence on the dominant role of Fc vs Fab in the acid-induced aggregation process. Natively purified Fc and Fab fragments of IgG2-A (see Materials and Methods) were mixed with the intact antibody and subjected to the pH 3.5 "high-salt" conditions detailed earlier. Figure 5 provides a summary of their aggregation kinetics in the acetate and citrate buffers. It is evident that the Fab region is remarkably resistant to aggregation, whereas the loss of Fc is almost identical to the loss of the full-length mAb irrespective of the buffer used. Clearly, Fc instability is likely to be the main driver behind IgG2-A aggregation under strongly acidic conditions. These results supported our hypothesis that IgG2 mAb aggregation at pH 3.5 may be controlled by the C_H2 domains located in the Fc region.

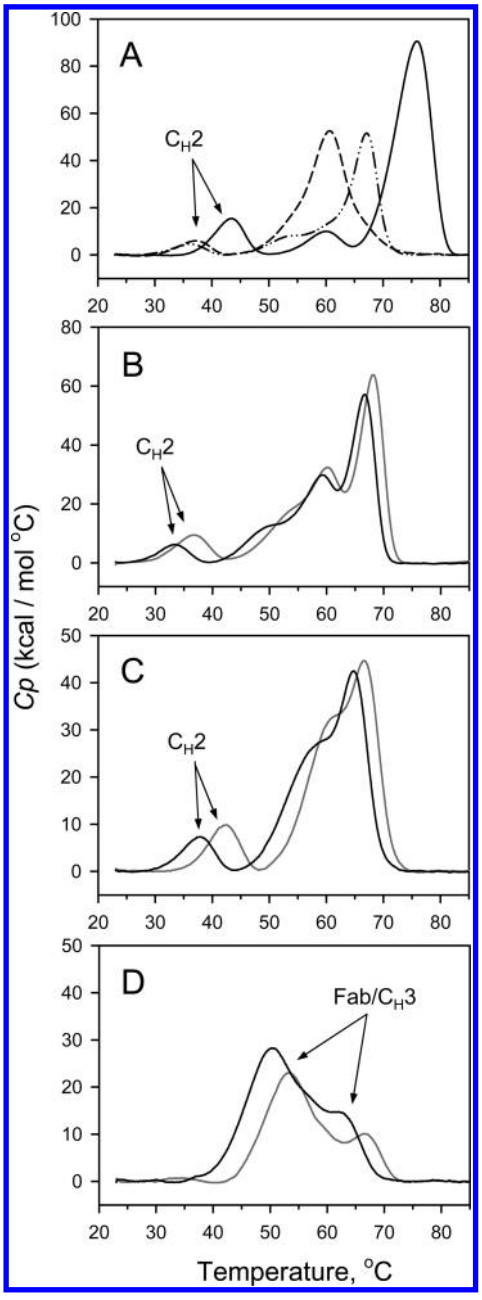

FIGURE 4: (A) DSC thermograms of IgG1-A (solid line), IgG2-A (dashed line), and IgG2-B (dashed and dotted line) at pH 3.5 in 50 mM acetic acid in the presence of 0.5 M NaCl. Note the characteristic differences in the C_H2 melting transitions between IgG1 and IgG2 mAbs. (B−D) DSC thermograms for IgG2-G (B), IgG2-F (C), and aglyco-IgG1 (D) in pH 3.5 acetic acid (50 mM) or citric acid (5 mM) solutions in the presence of 0.5 M NaCl. The acetic acid and citric acid data are shown in black and gray, respectively.

Aggregation Kinetics of the Fc and Fab Fragments of Aglyco-IgG1 at pH 3.5. The use of an aglycosylated IgG1 allowed an alternative assessment of the role of C_H2 instability in low pH mAb aggregation. Aglyco-IgG1 was the only IgG1 which aggregated dramatically at pH 3.5 in the presence of salt (see Figure 2). To assess whether this was a direct consequence of C_H2 destabilization (due to the removal of N-glycosylation), aggregation of its Fc and Fab fragments was investigated. In addition, a fully glycosylated variant of this antibody was prepared and used as a control. Native Fc and Fab were generated by limited proteolysis with Lys-C (see Materials and Methods) and incubated under high-salt conditions at pH 3.5. Figure 6 compares the

Table 2: C_H2 Domain Melting Transitions from DSC Measurements at pH 3.5 in the Presence of 0.5 M NaCl

antibody	IgG subclass	buffering agent[a]	T_m[b]	ΔT_m[c]
IgG1-A	IgG1	A	43.5	3.8
		C	47.3	
IgG1-B	IgG1	A	41.0	5.0
		C	46.0	
IgG1-C	IgG1	A	44.2	2.9
		C	47.1	
IgG1-D	IgG1	A	44.6	3.5
		C	48.1	
IgG1-E	IgG1	A	39.7	2.8
		C	42.5	
aglyco-IgG1	IgG1	A	n/a[d]	
		C	n/a[d]	
	all IgG1s		42.6 ± 2.1[e] (46.2 ± 2.2)[f]	3.6 ± 0.9[g]
IgG2-A	IgG2	A	37.1	3.4
		C	40.5	
IgG2-B	IgG2	A	36.2	4.5
		C	40.7	
IgG2-C	IgG2	A	38.5	3.7
		C	42.2	
IgG2-D	IgG2	A	32.1	2.5
		C	34.6	
IgG2-E	IgG2	A	33.5	2.9
		C	36.4	
IgG2-F	IgG2	A	38.0	4.2
		C	42.2	
IgG2-G	IgG2	A	33.4	3.4
		C	36.8	
IgG2-H	IgG2	A	34.4	5.3
		C	39.7	
IgG2-I	IgG2	A	32.6	3.8
		C	36.4	
IgG2-J	IgG2	A	34.0	5.4
		C	39.4	
	all IgG2s		35.0 ± 2.3[e] (38.9 ± 2.7)[f]	3.9 ± 1.0[g]

[a]A and C denote 50 mM acetic acid or 5 mM citric acid, respectively. [b]Melting temperature of the C_H2 domain. [c]The difference in T_m values between acetate and citrate samples (see text). [d]The melting transition of the C_H2 domain was not present (see text). [e]The mean value and standard deviation of the C_H2 domain melting transition for acetate-buffered samples. [f]The mean value and standard deviation of the C_H2 domain melting transition for citrate-buffered samples. [g]The difference in mean value and standard deviation of the C_H2 domain melting transition between acetate- and citrate-buffered samples.

Fc and Fab data overlaid with the results for the corresponding intact mAbs. In contrast to the IgG2-A data shown in Figure 5, the Fab portion of these IgG1s was relatively unstable and aggregated upon incubation. Nevertheless, in the case of aglyco-IgG1 the loss of Fab occurred at a much slower rate compared to the loss of Fc (see Figure 6A). The latter aggregated rapidly in good agreement with the data for the full-length molecule. Figure 6B illustrates a remarkable decrease in the aggregation propensity of the Fc fragment (and the corresponding mAb) as a result of C_H2 glycosylation. It is evident that glycosylation resulted in a dramatic improvement in the aggregation resistance of the molecule. The Fc and Fab data in Figure 6 were generated in the presence of a higher acetic acid concentration (160 mM) compared to the intact mAbs (56 mM). In a subsequent section we discuss that higher acid concentrations tend to further accelerate mAb aggregation. Therefore, maintaining similar acid concentration in these experiments would only improve the correspondence between the Fc and the intact molecule data. Evidently, the

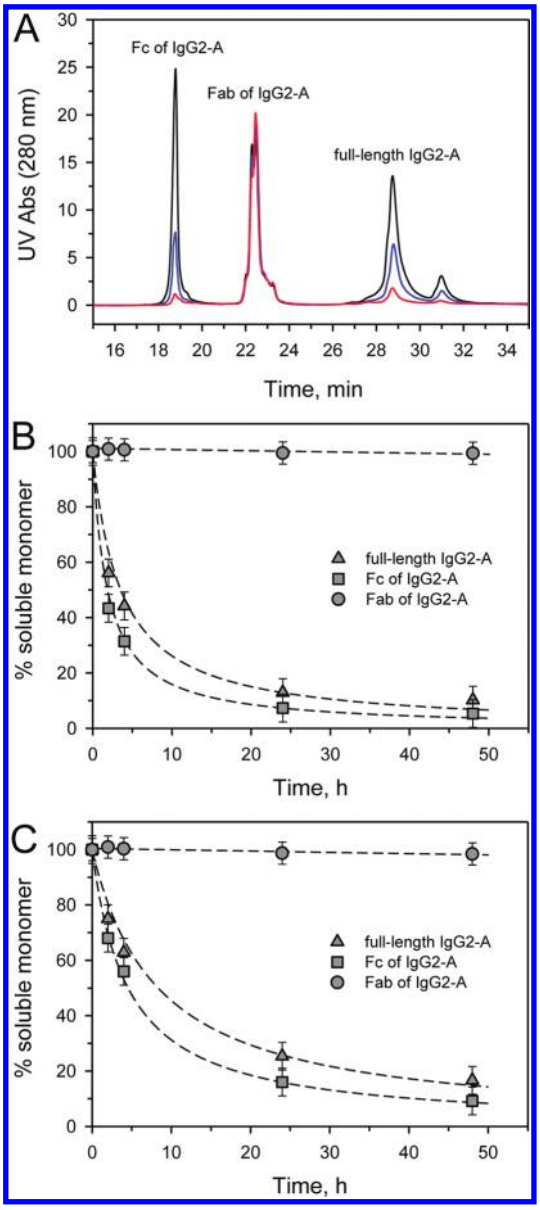

FIGURE 5: Coincubation experiments on IgG2-A and its Fc and Fab fragments. (A) CEX52 chromatographic overlays of samples incubated at pH 3.5 in the presence of 50 mM acetic acid and 0.5 M NaCl. The black, blue, and red traces correspond to 0, 4, and 24 h time points, respectively. The species eluting at ~31 min is part of the IgG2-A drug substance material (i.e., the full-length mAb). The kinetic data shown in (B) and (C) are generated at pH 3.5 in the presence of either 50 mM acetic acid and 0.5 M NaCl (B) or 5 mM citric acid and 0.5 M NaCl (C). Note the close correspondence between the loss of intact IgG2-A and its Fc fragment irrespective of the buffer system used. The error bars were calculated from the standard deviation of replicate injections over several runs. With the exception of the linear dashed line that was used to fit the Fab data, the dashed lines are model-dependent second-order fits (see Materials and Methods).

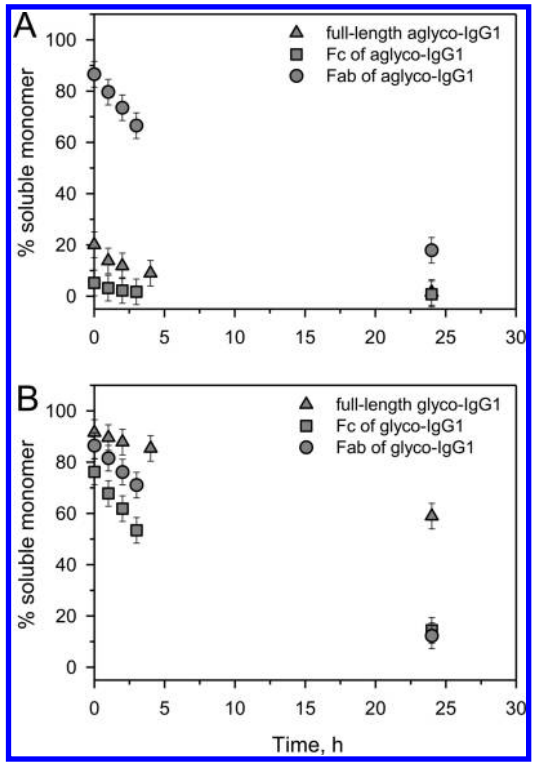

FIGURE 6: (A) Real-time aggregation of intact aglyco-IgG1 and its Fc and Fab fragments. (B) Real-time aggregation of a fully glycosylated variant of aglyco-IgG1 and its Fc and Fab fragments. The Fc and Fab fragments were coincubated in the absence of the intact mAbs to avoid the risk of residual protease activity (Lys-C was not removed via purification, but inhibited by DFP). The Fc and Fab data were generated at pH 3.5 in the presence of 160 mM acetic acid and 0.5 M NaCl, whereas aggregation of the intact IgGs was measured in the presence of 56 mM acetic acid and 0.5 M NaCl. The higher acetic acid concentration used in the case of the Fc and Fab experiments was needed to acidify Tris-HCl (pH 7.5) used during limited proteolysis (see Materials and Methods). Note the close correspondence between the loss of the intact aglyco-IgG1 and its Fc fragment in (A). The error bars were calculated from the standard deviation of replicate injections over several runs. No kinetic fitting was performed because only limited data were collected due to material constraints.

instability of the aglycosylated Fc (and its constituent C_H2 domain) made aglyco-IgG1 extremely susceptible to low pH aggregation. This illustrated that the leading role of C_H2 instability in low pH mAb aggregation was not limited to the IgG2 subclass. Rather, it was determined by the relative instability of the C_H2 domain with respect to other antibody domains.

Due to the slower but substantial loss of Fab, aglyco-IgG1 represented a case where Fab regions could potentially influence the aggregation process. This made it a useful model for cross-correlating DSC results with CEX52 aggregation data. As seen in Figure 4D, at pH 3.5 aglyco-IgG1 lacks the C_H2-related melting transition, suggesting that under the "high-salt" conditions the aglycosylated C_H2 domain is denatured. This can explain the unusually rapid aggregation of Fc and corresponding full-length molecule (Figure 6A). However, its Fab/C_H3 profile is also shifted to lower temperatures compared to other mAbs and partly overlaps with their C_H2 transitions (cf. Figure 4). Nevertheless, our results demonstrate that aglyco-IgG1 Fab regions have little effect at pH 3.5 where aggregation is strongly dominated by the C_H2-related pathway. Aggregation of this IgG1 becomes more Fab-dependent only when the Fc portion is glycosylated, which brings its stability closer to that of Fab. This may explain why the glycosylated form of this molecule shows some aggregation under conditions where most of the IgG1s are stable (cf. IgG1 data in Figures 3 and 6B). In addition, it suggests that the Fab-related pathway may become dominant in the cases where C_H2 stability exceeds that of Fab.

The results for aglyco-IgG1 illustrate the importance of calorimetrically determined stability in predicting the rate and mechanism of antibody aggregation. However, practical limitations of DSC may reduce the utility of such analysis. Identifying

and resolving multiple thermal transitions associated with various IgG domains can be problematic (Figure 4). It is also still unclear where the stability threshold is for nonnative aggregation or how different the domain stability must be for determining a single vs multipathway (multidomain) aggregation mechanism. Fortunately, IgG aggregation can be studied more easily by employing the CEX52-based methodology as described here (see also Chen et al. (*22*)). CEX52 offers a very simple and reliable measure of protein aggregation propensity, which could benefit structural and thermodynamic analysis of mAbs.

Mechanism of mAb Aggregation at pH 3.5. To gain further insight into the mechanism of low pH mAb aggregation, kinetic modeling was performed on the IgG2-A intact mAb and Fc data shown in Figures 5B,C. These data were inconsistent with the first-order aggregation model but were in close agreement with the second-order process, indicating that association of unfolded molecules or the growth of aggregates was the rate-limiting step in the aggregation process (*5*, *24*). Association-limited aggregation is characterized by relatively slow assembly steps leading to aggregation (*5*). In the case of equine IgG, aggregation at pH 3.4 was found to be diffusion limited and strongly dependent on the ionic strength (*14*). Apparently, the electrostatic repulsion at pH 3.4 was essentially negated already at moderate ionic strength (m = 0.27 M). In combination with protein denaturation at reduced pH, this resulted in an aggregation process controlled by protein−protein association rather than unfolding. Consistent with these earlier observations, aggregation profiles of IgG2s appeared to be linear in $1/[N] - 1/100$ versus t plots, reflecting the second-order process (see below). Whereas the second-order kinetics described our CEX data reasonably well, the first-order fits did not agree with the data quite as well. A combined first- and second-order analysis was also performed and indicated strong dominance of the second-order process (the first-order kinetic term was negligible compared to the second-order term). Therefore, we found that under the "high-salt" conditions pseudo-second-order kinetic modeling was appropriate.

Association-limited aggregation is expected to be controlled by the total monomer concentration (*5*). The effect of protein concentration on the rate of IgG2-B aggregation was tested in separate experiments at pH 3.7 (see Materials and Methods). It was observed that between 0.5 and 5.0 mg/mL the extent of IgG2-B aggregation was proportional to protein concentration. Samples containing 3.0 and 5.0 mg/mL protein were assessed only qualitatively as they aggregated already during preparation. In contrast, 0.5 and 1.0 mg/mL samples provided high quality data suitable for global fitting analysis. Once again, the first-order kinetics did not fit the data quite as well as the second-order aggregation model. The combined first- and second-order kinetics did fit the data but showed strong dominance of the second-order process. Global fitting of the 0.5 and 1.0 mg/mL data using the second-order kinetic model yielded a single rate constant of 0.0812 ± 0.0013 $(mg/mL)^{-1}$ h^{-1} (see Figure 7). This provided further evidence for the dominance of association-limited aggregation under the experimental conditions (a more detailed analysis of mAb aggregation kinetics will be presented elsewhere).

Identifying the IgG domains responsible for aggregation is important from a fundamental and practical perspective. Antibody aggregation has a complex temperature-, surface- and solution-dependent (i.e., pH, buffer, salts, etc.) character which explains the diversity of observed aggregation pathways (*22*). Considering

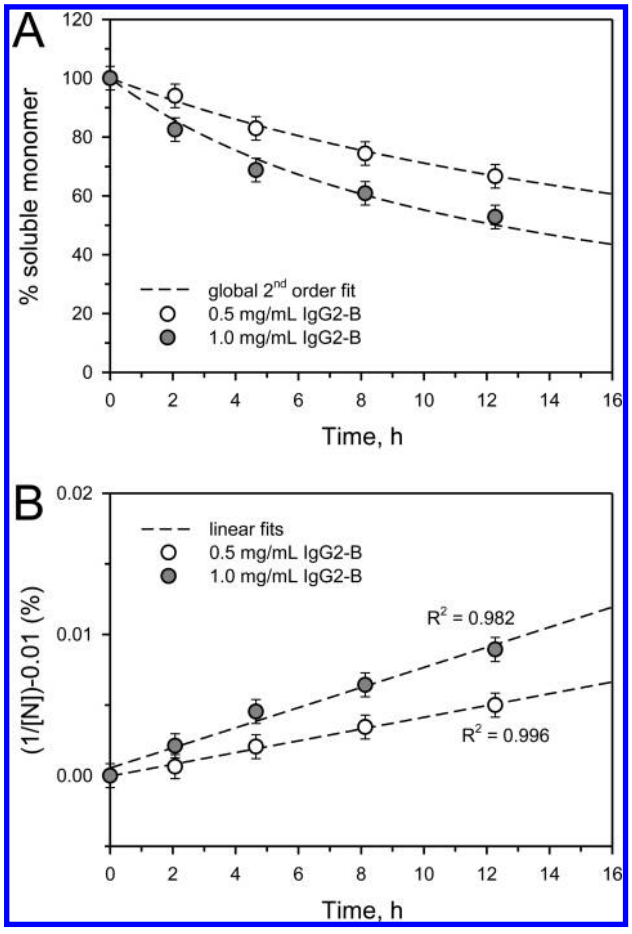

FIGURE 7: Protein concentration dependence of IgG2-B aggregation at pH 3.7 and 25 °C. Between 0.5 and 5.0 mg/mL the extent of IgG2-B aggregation was proportional to protein concentration. (A) Aggregation results corresponding to 0.5 and 1.0 mg/mL samples which provided high quality data for global fitting analysis (dashed lines). The data were fitted using the second-order kinetic model with a single rate constant of 0.0812 ± 0.0013 $(mg/mL)^{-1}$ h^{-1}. (B) Examples of the corresponding $1/[N] - 1/100$ versus t plots which appear linear in agreement with the second-order process (see Results and Discussion). The error bars were calculated from the standard deviation of replicate injections over several runs.

the large variety of current and future mAb-based therapeutics, it seems extremely unlikely that there is a single antibody aggregation mechanism. Our results do not support generalizations regarding the leading role of Fab over Fc (*31*) or vice versa. As the present study shows, unstable Fc regions (specifically, the C_H2 domains) clearly take precedence over Fab regions in low pH aggregation. However, the importance of Fab regions is indisputable in some other cases involving neutral pH conditions (*21*, *22*). Evidently, successful development of stable mAb-based therapeutics requires appropriate stabilization of both Fc and Fab regions.

Sequence Determinants of IgG2 C_H2 Instability at Low pH. With the exception of the hinge region, the Fc portions of IgG1 and IgG2 mAbs are very similar in both primary and tertiary structure. Table 3 lists the residue positions that are different between the C_H2 and C_H3 domains of IgG1s and IgG2s (in Eu numbering (*32*)). Sequence variations in the C_H2 domains are more numerous than in the C_H3 domains, but only one of them involves a charged residue: $K_{IgG1}274Q_{IgG2}$. Another notable charge variation is located in the hinge region preceding the C_H2 domain: $E_{IgG1}233P_{IgG2}$. Although the corresponding positions

Table 3: Residue Positions That Differ between the Hinge Region and the C_H2 and C_H3 Domains of IgG1 and IgG2 mAbs

	hinge region		C_H2 domain		C_H3 domain	
residue position(s)[a]	IgG1	IgG2	IgG1	IgG2	IgG1	IgG2
233−236	ELLG	PVA*[b]				
274			K	Q		
296			Y	F		
300			Y	F		
309			L	V		
327			A	G		
339			A	T		
356					D(E)[c]	E
358					L(M)[d]	M
397					V	M

[a]Residue numbering is listed in Eu format (*32*). [b]Missing residues (deletions) are indicated by an asterisk. [c]Some IgG1 mAbs contain Glu at this position. [d]Some IgG1 mAbs contain Met at this position.

are structurally distant (PBD entry 1HZH), it is possible that the ionization states of E233 and K274 play some role in aggregation. $Y_{IgG1}300F_{IgG2}$ is another substitution which could potentially affect IgG2 C_H2 stability. The Y(F)300 side chain is packed against H268, R292, and E294. At pH ~5, H268 and E294 may engage in charge−charge interactions stabilizing the domain. Under more acidic conditions, this interaction may be lost because of E294 protonation (theoretical pK_a = 4.07), potentially reflecting a pH sensitivity of the domain (*29*, *30*). Under such conditions, Y300, unlike F300, may form a hydrogen bond with H268 and preserve the folded structure. Alternatively, the difference in C_H2 domain stability may be caused by variations in core packing interactions. Site-specific mutagenesis experiments are currently ongoing to evaluate these hypotheses.

It is interesting to note that the human IgG1 C_H2 domain was found to be significantly more stable than the murine IgG1 C_H2 domain, and this phenomenon was explained by the differences in their amino acid sequences (*33*). These sequence disparities included most of the residue variations between the human IgG1 and IgG2 C_H2 domains (see Table 3). In fact, the sequence and stability of the murine IgG1 C_H2 domain appear to resemble more closely those of the human IgG2 C_H2 domain compared to the human IgG1 C_H2 domain, thus lending support to our observations.

Low pH mAb Aggregation Is Controlled by Ionic Strength and Total Acid Concentration. It has been recognized that ion−protein interactions can modulate aggregation and self-association of proteins (*34*−*40*). Nevertheless, the effect of ions on the extent and specificity of mAb aggregation is still poorly understood. It is common practice to perform acid treatment and neutralization of mAbs in the presence of 0.3−0.5 M salt. As this work demonstrates, salts and other ions are major accelerating factors of IgG2 aggregation at acidic pH. The role of salts in reducing the charge repulsion through Debye−Hückel screening effects and anion binding has been reviewed previously (*41*). The resulting stabilization of partially folded intermediates was reported for different proteins (*12*, *16*, *41*−*47*). Therefore, a careful examination of viral inactivation procedures is necessary for reducing the occurrence of aggregation-competent species. Optimization of subsequent neutralization steps would further decrease the risk of antibody aggregation during manufacturing (*7*, *12*, *15*).

Another important factor identified here is buffer selection. We investigated two buffers, acetate and citrate, commonly used in antibody manufacturing including the viral inactivation step. Interestingly, the extent and the rate of mAb aggregation in acetate and citrate samples were different despite similar pH and incubation conditions (see, for example, IgG2-F in Figure 2 and results for intact IgG2-A and its fragments in Figure 5B,C). Citrate samples showed less aggregation, an observation which held true for all ten IgG2s. In agreement with these results was the determined thermal stability of the mAbs, which was higher in citrate compared to acetate (Figure 4B−D and Table 2). Specifically, the average T_m of the IgG1 C_H2 domains was higher in citrate by 3.6 ± 0.9 °C. The corresponding difference for the IgG2 C_H2 domains was 3.9 ± 1.0 °C. Moreover, this effect was not limited to the C_H2 domains as qualitatively similar observations were made with respect to other domains (Figure 4B−D). These findings corroborated previous reports on the role of acid anions in decreasing the structural stability of IgGs (*48*).

We recognized the disparity between samples adjusted with 50 mM acetic acid and those using only 5 mM citric acid. In order to evaluate the role of acid concentration, an experiment was set up in which the citric acid level was raised from 5 to 50 mM. A control experiment was also performed in which the citric acid was maintained at 5 mM, but the NaCl concentration was raised by 45 mM. Protein mixture 5 was selected for these experiments (Figure 1B). As expected, the IgG1s (IgG1-A and IgG1-B) showed little to no aggregation after 2 days of incubation at pH 3.5, whereas both IgG2s (IgG2-B and IgG2-C) aggregated significantly (see Figure 8). Once again, the standard 5 mM citrate sample aggregated less dramatically than its 50 mM acetate-based counterpart (cf. white circles and black triangles in panels A and B of Figure 8, as well as white and black bars in Figure 8C). However, the additional citric acid promoted aggregation to an extent comparable to equimolar acetate (see dark gray symbols and bars in Figure 8). In contrast, the addition of 45 mM NaCl, accounting for only ~10% of the total ionic strength, did not greatly influence the process since all samples already contained 0.5 M NaCl (light gray symbols and bars in Figure 8).

An important conclusion that can be drawn from these experiments is that acid concentration is another key factor in determining the extent of low pH mAb aggregation. Therefore, we recommend using acids at low concentrations throughout the IgG manufacturing process and especially during the viral inactivation step. The data also indicate that acids can substantially affect proteins through mechanisms that differ from Debye−Hückel screening effects and must involve more specific binding interactions (*41*, *42*, *44*). Fortunately, these effects are effectively negated by the increased charge−charge repulsion between proteins at low pH and reduced salt concentrations. As our experiments demonstrate, there are no significant differences in aggregation between samples with 5 mM citric acid and those with 50 mM acetic acid in the absence of 0.5 M NaCl (cf. IgG2-F low- and high-salt data in Figure 2).

Currently, our understanding regarding the effects of acids on antibody stability and aggregation is incomplete. It is recognized that the effects of pH and salt on the extent of acid ionization should be taken into account. Our findings resemble earlier observations that an increase in acetic acid concentration accelerated egg albumin denaturation and aggregation (*49*). Specifically, higher acetic acid concentrations allowed protein destabilization to occur at higher (less denaturing) pH values. It was also considered that the increased rate of denaturation resulted from the presence of un-ionized acetic acid (*49*). A similar scenario may be playing out in our pH 3.5 experiments in which the acetic acid

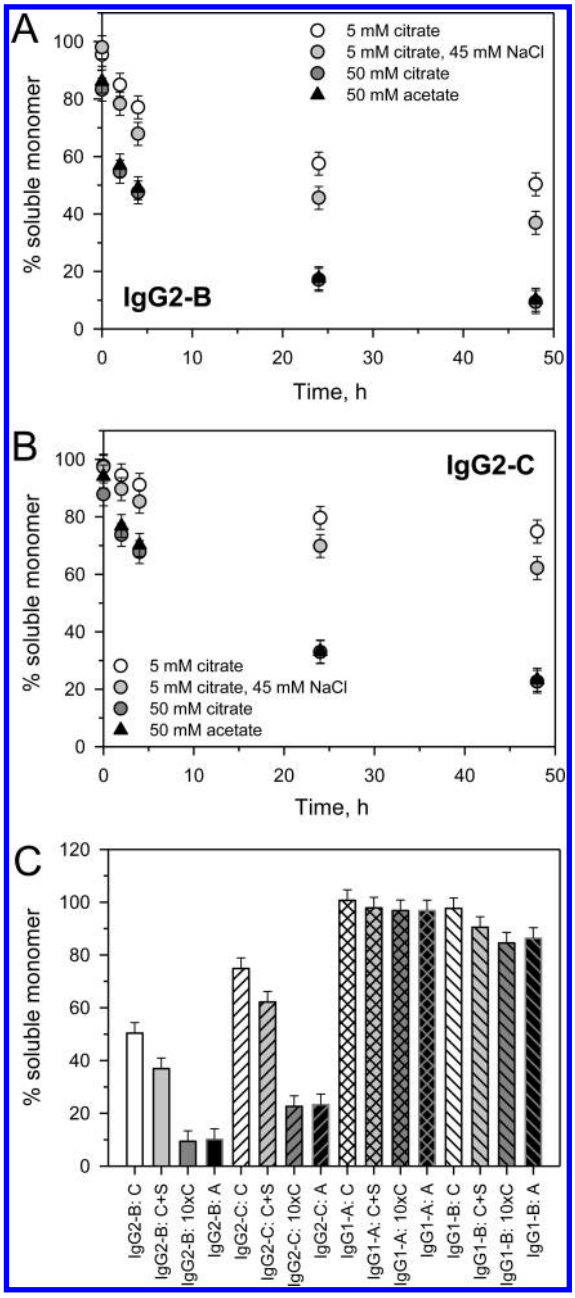

FIGURE 8: The effect of acid concentration on low pH mAb aggregation in the case of mixture 5 (see also Figure 1B and Table 1). Real-time aggregation of IgG2-B and IgG2-C is shown in (A) and (B), respectively. (C) Percent remaining soluble monomer after 48 h at pH 3.5 and 25 °C for the four mAbs comprising mixture 5. The four buffer conditions tested were 5 mM citric acid (white), 5 mM citric acid with an additional 45 mM NaCl (gray), 50 mM citric acid (dark gray), and 50 mM acetic acid (black). Note that all samples contained at least 0.5 M NaCl to accelerate antibody aggregation. In (C) citric acid is denoted as C, NaCl as S (salt), and acetic acid as A. The error bars were calculated from the standard deviation of replicate injections over several runs.

is expected to be largely protonated (pK_a = 4.76). However, this does not explain comparable aggregation accelerating effect of citric acid (pK_a = 3.13) at the same molar concentration. It is known that anions may participate in ion-pairing interactions which preferentially stabilize aggregation-prone conformations (the A-state) of mAbs (*12*, *16*). Particularly, the Fab fragment and the C_H3 domain were shown to adopt an alternatively folded state at acidic pH values and low to moderate ionic strength (*13*, *16*). Similar conclusions were made on the role of anion binding in modulating low pH conformations of other proteins (*41*, *44*, *47*). Importantly, the order of effectiveness of various anions in stabilizing the A-state followed their electroselectivity series toward the anion-exchange resin (*41*, *42*, *50*, *51*). A more detailed analysis of acid effects on antibody stability and aggregation will be presented elsewhere.

CONCLUSIONS

The CEX52 methodology provides a rare insight into the complex mechanism controlling aggregation of such multidomain proteins as IgG antibodies. The rate and extent of low pH mAb aggregation are shown to be strongly dependent on the antibody subclass (IgG1 vs IgG2). It is evident that IgG2s are less stable than IgG1s and aggregate more readily at pH 3.5 in the presence of salt. The ionic strength and total acid concentration of the solution play a major role in mAb aggregation under acidic conditions. We postulate that acid-induced aggregation of typical IgG2s proceeds predominantly via a C_H2-related aggregation pathway.

ACKNOWLEDGMENT

The authors thank Yan Brodsky, Stephen P. Trimble, Shabnam Farahmand, Laurie Jones, Robert Bailey, Gerd R. Kleemann, Linda O. Narhi, Michael J. Treuheit, Dean Pettit, and David N. Brems for assistance and fruitful discussions.

REFERENCES

1. Wang, Y. J., and Hanson, M. A. (1988) Parenteral formulations of proteins and peptides: stability and stabilizers. *J. Parenter. Sci. Technol. 42*, 453–525.
2. Cleland, J. L., Powell, M. F., and Shire, S. J. (1993) The development of stable protein formulations: a close look at protein aggregation, deamidation, and oxidation. *Crit. Rev. Ther. Drug Carrier Syst. 10*, 307–377.
3. Wang, W. (2005) Protein aggregation and its inhibition in biopharmaceutics. *Int. J. Pharm. 289*, 1–30.
4. Cromwell, M. E., Hilario, E., and Jacobson, F. (2006) Protein aggregation and bioprocessing. *AAPS J. 8*, E572–E579.
5. Weiss, W. F., IV, Young, T. M., and Roberts, C. J. (2009) Principles, approaches, and challenges for predicting protein aggregation rates and shelf life. *J. Pharm. Sci. 98*, 1246–1277.
6. Manning, M. C., Chou, D. K., Murphy, B. M., Payne, R. W., and Katayama, D. S. (2010) Stability of protein pharmaceuticals: an update. *Pharm. Res. 27*, 544–575.
7. Ejima, D., Tsumoto, K., Fukada, H., Yumioka, R., Nagase, K., Arakawa, T., and Philo, J. S. (2007) Effects of acid exposure on the conformation, stability, and aggregation of monoclonal antibodies. *Proteins 66*, 954–962.
8. Harris, R. J., Kabakoff, B., Macchi, F. D., Shen, F. J., Kwong, M., Andya, J. D., Shire, S. J., Bjork, N., Totpal, K., and Chen, A. B. (2001) Identification of multiple sources of charge heterogeneity in a recombinant antibody. *J. Chromatogr., B: Biomed. Sci. Appl. 752*, 233–245.
9. Johnson, K. A., Paisley-Flango, K., Tangarone, B. S., Porter, T. J., and Rouse, J. C. (2007) Cation exchange−HPLC and mass spectrometry reveal C-terminal amidation of an IgG1 heavy chain. *Anal. Biochem. 360*, 75–83.
10. Wypych, J., Li, M., Guo, A., Zhang, Z., Martinez, T., Allen, M. J., Fodor, S., Kelner, D. N., Flynn, G. C., Liu, Y. D., Bondarenko, P. V., Ricci, M. S., Dillon, T. M., and Balland, A. (2008) Human IgG2 antibodies display disulfide-mediated structural isoforms. *J. Biol. Chem. 283*, 16194–16205.
11. Dillon, T. M., Ricci, M. S., Vezina, C., Flynn, G. C., Liu, Y. D., Rehder, D. S., Plant, M., Henkle, B., Li, Y., Deechongkit, S., Varnum, B., Wypych, J., Balland, A., and Bondarenko, P. V. (2008) Structural and functional characterization of disulfide isoforms of the human IgG2 subclass. *J. Biol. Chem. 283*, 16206–16215.
12. Buchner, J., Renner, M., Lilie, H., Hinz, H. J., Jaenicke, R., Kiefhaber, T., and Rudolph, R. (1991) Alternatively folded states of an immunoglobulin. *Biochemistry 30*, 6922–6929.

13. Lilie, H., and Buchner, J. (1995) Domain interactions stabilize the alternatively folded state of an antibody Fab fragment. *FEBS Lett. 362*, 43–46.
14. Lewis, J. D., Ju, R. T-C., Kim, A. I., and Nail, S. L. (1997) Kinetics of low pH induced aggregation of equine IgG. *J. Colloid Interface Sci. 196*, 170–176.
15. Welfle, K., Misselwitz, R., Hausdorf, G., Höhne, W., and Welfle, H. (1999) Conformation, pH-induced conformational changes, and thermal unfolding of anti-p24 (HIV-1) monoclonal antibody CB4-1 and its Fab and Fc fragments. *Biochim. Biophys. Acta 1431*, 120–131.
16. Thies, M. J., Kammermeier, R., Richter, K., and Buchner, J. (2001) The alternatively folded state of the antibody C_H3 domain. *J. Mol. Biol. 309*, 1077–1085.
17. Kameoka, D., Masuzaki, E., Ueda, T., and Imoto, T. (2007) Effect of buffer species on the unfolding and the aggregation of humanized IgG. *J. Biochem. 142*, 383–391.
18. Ishikawa, T., Ito, T., Endo, R., Nakagawa, K., Sawa, E., and Wakamatsu, K. (2010) Influence of pH on heat-induced aggregation and degradation of therapeutic monoclonal antibodies. *Biol. Pharm. Bull. 33*, 1413–1417.
19. Franey, H., Brych, S. R., Kolvenbach, C. G., and Rajan, R. S. (2010) Increased aggregation propensity of IgG2 subclass over IgG1: role of conformational changes and covalent character in isolated aggregates. *Protein Sci. 19*, 1601–1615.
20. Sahin, E., Grillo, A. O., Perkins, M. D., and Roberts, C. J. (2010) Comparative effects of pH and ionic strength on protein-protein interactions, unfolding, and aggregation for IgG1 antibodies. *J. Pharm. Sci.* (DOI: 10.1002/jps.22198).
21. Lau, H., Pace, D., Yan, B., McGrath, T., Smallwood, S., Patel, K., Park, J., Park, S. S., and Latypov, R. F. (2010) Investigation of degradation processes in IgG1 monoclonal antibodies by limited proteolysis coupled with weak cation-exchange HPLC. *J. Chromatogr., B: Anal. Technol. Biomed. Life Sci. 878*, 868–876.
22. Chen, S., Lau, H., Brodsky, Y., Kleemann, G. R., and Latypov, R. F. (2010) The use of native cation-exchange chromatography to study aggregation and phase separation of monoclonal antibodies. *Protein Sci. 19*, 1191–1204.
23. Kleemann, G. R., Beierle, J., Nichols, A. C., Dillon, T. M., Pipes, G. D., and Bondarenko, P. V. (2008) Characterization of IgG1 immunoglobulins and peptide-Fc fusion proteins by limited proteolysis in conjunction with LC-MS. *Anal. Chem. 80*, 2001–2009.
24. Roberts, C. J. (2006) Non-native protein aggregation: pathways, kinetics, and shelf-life prediction, in Misbehaving Proteins: Protein (Mis)folding, Aggregation, and Stability (Murphy, R. M., and Tsai, A., Eds.) pp 17−46, Springer, New York.
25. Roberts, C. J. (2003) Kinetics of irreversible protein aggregation: analysis of extended Lumry-Eyring models and implications for predicting protein shelf life. *J. Phys. Chem. B 107*, 1194–1207.
26. Roberts, C. J., Darrington, R. T., and Whitley, M. B. (2003) Irreversible aggregation of recombinant bovine granulocyte-colony stimulating factor (bG-CSF) and implications for predicting protein shelf life. *J. Pharm. Sci. 92*, 1095–1111.
27. Cordoba, A. J., Shyong, B.-J., Breen, D., and Harris, R. J. (2005) Non-enzymatic hinge region fragmentation of antibodies in solution. *J. Chromatogr., B: Anal. Technol. Biomed. Life Sci. 818*, 115–121.
28. Feige, M. J., Walter, S., and Buchner, J. (2004) Folding mechanism of the C_H2 antibody domain. *J. Mol. Biol. 344*, 107–118.
29. Tischenko, V. M., Zav'yalov, V. P., Medgyesi, G. A., Potekhin, S. A., and Privalov, P. L. (1982) A thermodynamic study of cooperative structures in rabbit immunoglobulin G. *Eur. J. Biochem. 126*, 517–521.
30. Vermeer, A. W., and Norde, W. (2000) The thermal stability of immunoglobulin: unfolding and aggregation of a multi-domain protein. *Biophys. J. 78*, 394–404.
31. Wang, L., and Ghosh, R. (2008) Fractionation of monoclonal antibody aggregates using membrane chromatography. *J. Membr. Sci. 318*, 311–316.
32. Edelman, G. M., Cunningham, B. A., Gall, W. E., Gottlieb, P. D., Rutishauser, U., and Waxdal, M. J. (1969) The covalent structure of an entire γG immunoglobulin molecule. *Proc. Natl. Acad. Sci. U.S.A. 63*, 78–85.
33. Gong, R., Vu, B. K., Feng, Y., Prieto, D. A., Dyba, M. A., Walsh, J. D., Prabakaran, P., Veenstra, T. D., Tarasov, S. G., Ishima, R., and Dimitrov, D. S. (2009) Engineered human antibody constant domains with increased stability. *J. Biol. Chem. 284*, 14203–14210.
34. Raibekas, A. A., Bures, E. J., Siska, C. C., Kohno, T., Latypov, R. F., and Kerwin, B. A. (2005) Anion binding and controlled aggregation of human interleukin-1 receptor antagonist. *Biochemistry 44*, 9871–9879.
35. Kanai, S., Liu, J., Patapoff, T. W., and Shire, S. J. (2008) Reversible self-association of a concentrated monoclonal antibody solution mediated by Fab-Fab interaction that impacts solution viscosity. *J. Pharm. Sci. 97*, 4219–4227.
36. Gokarn, Y. R., Fesinmeyer, R. M., Saluja, A., Cao, S., Dankberg, J., Goetze, A., Remmele, R. L., Jr., Narhi, L. O., and Brems, D. N. (2009) Ion-specific modulation of protein interactions: anion-induced, reversible oligomerization of a fusion protein. *Protein Sci. 18*, 169–179.
37. Esue, O., Kanai, S., Liu, J., Patapoff, T. W., and Shire, S. J. (2009) Carboxylate-dependent gelation of a monoclonal antibody. *Pharm. Res. 26*, 2478–2485.
38. Fesinmeyer, R. M., Hogan, S., Saluja, A., Brych, S. R., Kras, E., Narhi, L. O., Brems, D. N., and Gokarn, Y. R. (2009) Effect of ions on agitation- and temperature-induced aggregation reactions of antibodies. *Pharm. Res. 26*, 903–913.
39. Saluja, A., Crampton, S., Kras, E., Fesinmeyer, R. M., Remmele, R. L., Jr., Narhi, L. O., Brems, D. N., and Gokarn, Y. R. (2009) Anion binding mediated precipitation of a peptibody. *Pharm. Res. 26*, 152–160.
40. Yadav, S., Liu, J., Shire, S. J., and Kalonia, D. S. (2010) Specific interactions in high concentration antibody solutions resulting in high viscosity. *J. Pharm. Sci. 99*, 1152–1168.
41. Hamada, D., and Goto, Y. (2005) Alcohol- and salt-induced partially folded intermediates, in The Protein Folding Handbook (Buchner, J., and Kiefhaber, T., Eds.) pp 884−915, Wiley-VCH, Weinheim.
42. Goto, Y., Takahashi, N., and Fink, A. L. (1990) Mechanism of acid-induced folding of proteins. *Biochemistry 29*, 3480–3488.
43. Goto, Y., Calciano, L. J., and Fink, A. L. (1990) Acid-induced folding of proteins. *Proc. Natl. Acad. Sci. U.S.A. 87*, 573–577.
44. Fink, A. L., Calciano, L. J., Goto, Y., Kurotsu, T., and Palleros, D. R. (1994) Classification of acid denaturation of proteins: intermediates and unfolded states. *Biochemistry 33*, 12504–12511.
45. Fink, A. L. (1995) Compact intermediate states in protein folding. *Annu. Rev. Biophys. Biomol. Struct. 24*, 495–522.
46. Uversky, V. N., Karnoup, A. S., Segel, D. J., Seshadri, S., Doniach, S., and Fink, A. L. (1998) Anion-induced folding of staphylococcal nuclease: characterization of multiple equilibrium partially folded intermediates. *J. Mol. Biol. 278*, 879–894.
47. Uversky, V. N., and Goto, Y. (2009) Acid denaturation and anion-induced folding of globular proteins: multitude of equilibrium partially folded intermediates. *Curr. Protein Pept. Sci. 10*, 447–455.
48. Vlasov, A. P., Kravchuk, Z. I., and Martsev, S. P. (1996) Non-native conformational states of immunoglobulins: thermodynamic and functional studies of rabbit IgG. *Biochemistry* (*Moscow*) *61*, 155–171.
49. Bull, H. B., and Breese, K. (1967) Denaturation of proteins by fatty acids. *Arch. Biochem. Biophys. 120*, 309–315.
50. Gregor, H. P., Belle, J., and Marcus, R. A. (1955) Studies on ion-exchange resins. XIII. Selectivity coefficients of quaternary base anion exchange resins toward univalent anions. *J. Am. Chem. Soc. 77*, 2713–2719.
51. Gjerde, D. T., Schmuckler, G., and Fritz, J. S. (1980) Anion chromatography with low-conductivity eluents. II. *J. Chromatogr. A 187*, 35–45.